Available online at www.sciencedirect.com
SCIENCE DIRECT®
Electrochimica Acta 49 (2004) 2453–2460
ELECTROCHIMICA Acta
www.elsevier.com/locate/electacta

Supramolecular assembly of porphyrin bound DNA and its catalytic behavior for nitric oxide reduction

Jianping Lei [a], Huangxian Ju [b], Osamu Ikeda [a,*]

[a] *Department of Chemistry, Faculty of Science, Kanazawa University, General Education Hall, Kakuma, Kanazawa, Ishikawa 920-1192, Japan*
[b] *State Key Laboratory of Coordination Chemistry, Department of Chemistry, Institute of Chemical Biology, Nanjing University, Nanjing 210093, PR China*

Received 8 October 2003; received in revised form 25 November 2003; accepted 27 January 2004

Abstract

A stable Fe(4-TMPyP)-DNA-PADDA (FePyDP) film was prepared on pyrolytic graphite electrode (PGE) through the supramolecular interaction between water-soluble iron(III) meso-tetrakis(*N*-methylpyridinium-4-yl)porphyrin (Fe(4-TMPyP)) and DNA template, where PADDA (poly(acrylamide-*co*-diallyldimethylammonium chloride)) is employed as a co-immobilizing polymer. Electronic absorption spectral and quartz crystal microbalance measurements revealed that Fe(4-TMPyP) interacted with DNA to generate a species with the molar ratio of 1:5 for Fe(4-TMPyP):DNA phosphate. Cyclic voltammetry of FePyDP film showed a pair of stable and reversible peaks corresponding to Fe^{III}/Fe^{II} redox potential of −0.13 V versus Ag|AgCl in pH 7.4 PBS. The electron transfer was expected across the double-strand of DNA by an "electron tunneling" mechanism. The modified electrode displayed an excellent catalytic activity for NO reduction at −0.61 V versus Ag|AgCl. The catalytic current was enhanced at lower pH. Chronoamperometric experiments demonstrated a rapid response to the reduction of NO with a linear range from 0.1 to 90 μM. The detection limit was 30 nM at a signal-to-noise ratio of 3.

Keywords: Supramolecular assembly; Porphyrin bound DNA; Nitric oxide reduction; Electrocatalysis; Modified electrode

1. Introduction

Nitric oxide has been known to be an intercellular signaling agent in a diverse array of biological systems [1–3]. The need for measurement of a small amount of NO has led to the development of various analytical methods. Among those methods, electrochemical methods are the most promising. Since Malinski and Taha [4] reported the application of an electropolymerized nickel porphyrin film electrode for the detection of NO, the metalloporphyrin biosensor has intensively been investigated for amperometric measurements of NO [5–11]. The methods for the immobilization of metalloporphyrins on the electrode surface include electropolymerization of metalloporphyrins [5,6], polypyrrole doping with metalloporphyrins [7,8] and deposition of metalloporphyrins entrapped in Nafion film [9–11]. In order to obtain better analytical performance of the electrochemical NO sensors, it is a great deal to develop new materials for incorporating porphyrin on electrode surfaces. In this context, we prepared a novel porphyrin film, Fe(4-TMPyP)-DNA-PADDA (FePyDP) film, through the supramolecular assembly of cationic porphyrins into DNA template and developed a new NO sensor.

The study on the supramolecular interaction of cationic porphyrins and their derivatives with DNA is of considerable interest due to their potential applications as biological materials and probes for nucleic acid structure and dynamics. Three major modes have been proposed for the binding of cationic porphyrins with DNA: intercalation, outside binding without self-stacking, and outside binding with self-stacking along the nucleic acids surface [12,13]. The binding of porphyrin with DNA is presumably stabilized by electrostatic interaction between the positively charged substituent on the porphyrin periphery and the negatively charged phosphate group of DNA. In the case of intercalation, a favorable aromatic π–π stacking interaction between the porphyrin macrocycle and the base pair of nucleic acid is also involved [14]. Circular dichroism spectrum suggested that H_2TMPyP was predominantly intercalated into the GC sites at a water-insoluble layer-by-layer DNA/PAH film [15].

* Corresponding author. Fax: +81-76-264-5988.
E-mail address: osamu@kenroku.kanazawa-u.ac.jp (O. Ikeda).

0013-4686/$ – see front matter © 2004 Elsevier Ltd. All rights reserved.
doi:10.1016/j.electacta.2004.01.023

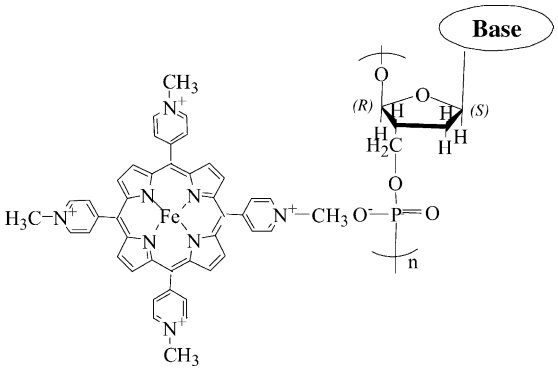

Fig. 1. Chemical structure of Fe(4-TMPyP) bound DNA.

On the other hand, DNA film has been used as an electroconductive biological film [16,17]. Giese and Biland [16] suggested a multistep hopping mechanism for the long distance charge migration along the double-strand of DNA. Okahata and coworkers [17] directly observed the switchable electron conduction along intramolecular DNA strands by using DNA-lipid cast film on a comb-type electrode. Especially, the introduction of redox-active complexes into the double helix of DNA is envisioned for development of new biomaterials or efficient redox systems [18]. Kelley et al. [19] reported a long-range electron transfer across oriented ds-DNA monolayer in which daunomycin was covalently bound to the G residues. A unimolecular intra-complex electron transfer has been found in an ion-pair complex between cationic porphyrins and anionic oligopeptides [20]. Recently, Rusling and coworkers [21,22] prepared a new type of biomembrane-like film, an ordered multibilayer polyion-surfactant/DNA composite film, and studied its electron transfer behavior. It is significant in the point that the direct electron transfer between redox protein and electrode can be realized for preparation of reagentless biosensor without help of any mediator.

Our previous research has demonstrated that the reaction of iron(III) meso-tetrakis(*N*-methylpyridinium-4-yl) porphyrin (Fe(4-TMPyP)) with NO undergoes a reductive nitrosylation in aqueous solutions in a wide pH range [23]. In this work, a stable FePyDP film was prepared by supramolecular interaction between Fe(4-TMPyP) and DNA template, and the catalytic activity of the resulting film towards NO reduction was investigated. The interaction between positively charged Fe(4-TMPyP) and negatively charged DNA template is expected to form a stable complex of DNA-bound-porphyrin as shown in Fig. 1.

2. Experimental

2.1. Chemicals

Fe^{III}(4-TMPyP) was prepared according to the methods suggested by Pasternack et al. [24] and Bedioui et al. [25]. The product was purified by chromatography with help of anion exchange resin. Salmon testis double strand (ST-ds) DNA (Sigma), poly(acrylamide-*co*-diallyldimethylammonium chloride) (PADDA, Aldrich), and poly(vinyl sulfonate), (PVS, Polysciences) were used as received. DNA concentration was estimated in nucleotide phosphate, which was determined using spectrophotometer with ε of 1.31×10^4 $M^{-1}\,cm^{-1}$ at 260 nm [12].

Phosphate buffer solutions (PBS, 50 mM) with a wide range of pH were prepared by mixing 50 mM solutions of KOH, KH_2PO_4 and K_2HPO_4 (Wako, analytical grade). The solution pH was monitored using a digital pH meter (TOA, HM-30V). All aqueous solutions were prepared with twice distilled water.

All solutions were deoxygenated by bubbling ultrapure argon gas (Nippon Sanso, 99.9999%) for 20 min. NO-saturated solution was prepared by bubbling mixed gas of 5% NO and 95% Ar (Nippon Sanso) for 30 min into a deoxygenated solution before each electrochemical and spectroscopic run. The NO gas mixture were purified from possible traces of high-valent nitrogen oxides and dioxygen by passing through three successive vials containing a 10% solution of potassium hydroxide, an alkaline solution of pyrogallol, and pure water finally. The molar concentration of NO in solution was evaluated from Ostwald's solubility coefficient [26] for a given partial pressure of NO.

2.2. Preparation of DNA-PADDA composite and cast films

The mixture of 0.3 ml aqueous solution of 15 mg ml^{-1} ST-dsDNA and 0.2 ml aqueous solution of 15 mg ml^{-1} PADDA was set at a room temperature for 30 min until a white precipitate of DNA-PADDA was formed. After being set at ambient temperature overnight, the solution was centrifuged, and the sediment was washed with pure water and then dried at a room temperature. Such dried DNA-PADDA composite powder was dispersed in water by ultrasonication for 30 min to obtain a DNA-PADDA cloudy suspension of 3 mg ml^{-1}. Prior to casting the suspension was ultrasonicated for another 10 min.

Edge plane PGE was abraded with metallographic sandpaper (2000 grit) and then polished on a clean billiard cloths with 0.06 μm aluminum powder for about 3 min, followed by ultrasonicating in pure water for 2 min. Ten microliter 3 mg ml^{-1} DNA-PADDA suspension was cast on the cleaned electrode surface and dried in air overnight. After the electrode was soaked in water for at least 4 h and rinsed with water to remove any unadsorbed composite, one DNA-PADDA film modified PGE was obtained. The electrode was then immersed in 2×10^{-4} M Fe(4-TMPyP) solution for 60 min to prepare FePyDP film. A similar process was applied to indium tin oxide (ITO) transparent electrode for UV-Vis spectroscopy (Hitachi U2000).

2.3. Quartz crystal microbalance (QCM) measurements

The assembly process was monitored on a QCA917 type quartz crystal microbalance (SEIKO EG&G Co., Japan)

linked to a personal computer for the microgravimetric analysis. QCM crystals used for the quantification of immobilized Fe(4-TMPyP) were at 9 MHz. An AT-cut shear mode quartz crystal deposited gold on both sides with a geometric area of 0.2 cm^2 was used. A typical QCM experiment began from the cleaning of the Au/quartz crystal surface with a piranha solution (30% H_2O_2 and 70% concentrated H_2SO_4). *Caution: Piranha solution reacts violently with organic solvents and is a skin irritant. Extreme caution should be exercised when handling piranha solution*. After rinsing with twice-distilled water, the Au/quartz crystal was dried over a stream of N_2 gas. Following the same procedure as on PGE, a DNA-PADDA modified Au/quartz crystal electrode was prepared. The Au/quartz crystal electrode was sealed in an electrolytic cell with a Teflon casing, and one side was exposed to 2×10^{-4} M Fe(4-TMPyP) solution for in situ frequency measurements.

2.4. Electrochemical apparatus

Electrochemical data were collected with an electrochemical workstation (BAS, model 100B/W). Cyclic voltammetry (CV) experiments were carried out using a bare PGE (o.d., 5 mm; i.d., 3 mm) or FePyDP film modified PGE as the working electrode in a one-compartment three-electrode cell protected against air penetration. A platinum wire served as a counter electrode, and an Ag|AgCl|3 M NaCl reference electrode, to which all reported potentials were referenced, were employed.

2.5. Characteristics of DNA-PADDA film

In order to prepare DNA-PADDA film coated electrode, PGE or ITO with a surface area of 0.20 cm^2 were uniformly covered with 10 μl of 3 mg ml^{-1} DNA-PADDA suspension and then dried at a room temperature. A thickness of DNA-PADDA film was evaluated to be (1.2 ± 0.1 μm) by taking into account (1.2 ± 0.1 g cm^{-3}) as the density of polyions [27,28]. The ratio of negative charges on DNA to positive charges on PADDA in the film was estimated to be 1.7 by using initial mixing ratio of DNA to PADDA and the composition of polyacrylamide (55 wt.%) and poly(diallyldimethylammonium chloride) (45 wt.%) in the co-immobilizing polymer, PADDA. This result indicated that the film had excess negative charges and 40% of negative charges on DNA are usable for an interaction with positively charged species.

3. Results and discussion

3.1. Interaction between Fe(4-TMPyP) and DNA

The interaction of Fe(4-TMPyP) to DNA was monitored from the corresponding DNA-induced changes on the UV-Vis absorption by addition of the DNA stock solution into a cuvette containing 5 μM iron porphyrin. Upon initial addition of DNA, the intensity of the Soret band of iron porphyrin decreased and the λ_{max} slightly red-shifted (Fig. 2A). In Q band region a new absorption peak was clearly observed at 565 nm with three isosbestic points at 552, 582 and 660 nm. This result suggested that a bound I complex was formed by binding of positively charged porphyrin to DNA with a molar ratio of 1:1.6 for Fe(4-TMPyP):DNA phosphate, and the main driving force should be nonspecific electrostatic binding at low DNA concentration [29,30]. Kuroda and Tanaka [31] supposed that MnTMPyP could bind with the phosphate groups of AT and GC base pairs in the major groove of DNA double helix, as well as AT base pairs in the minor groove. With the increasing DNA concentration, the Soret band red-shifted to 428 nm and a new absorption peak appeared at 515 nm, which indicated that the interaction with porphyrin became more specific and bound I changed into other species (bound II) with the molar radio of 1:5 Fe(4-TMPyP):DNA phosphate in Fig. 2B. A theoretical study [32] have clarified that the binding in the DNA minor groove produced better steric conditions for the formation of porphyrin aggregates through π–π stacking interaction in comparison with those in the major one. In this sense, it was reasonable that the binding site of Fe(4-TMPyP) might be changed with the increase of DNA concentration and Fe(4-TMPyP) dislocated from the major groove to the minor groove, which was in good agreement with the observations in Fig. 2B. As the result, Fe(4-TMPyP) existed in the solution as three species: the uncomplexed porphyrin, bound I, and bound II depending on the DNA concentration.

Fig. 2C shows a plot of the absorbance at 422 nm (near the Soret maximum of the porphyrin in aqueous solution) versus nucleotide phosphate concentration of DNA. The plot showed clearly two stages in the process of interaction of Fe(4-TMPyP) with DNA. The binding constant, K, for the low and high DNA concentration ranges could be determined by Eq. (1) [29]:

$$\varepsilon_F - \varepsilon_A = \frac{\varepsilon_A - \varepsilon_F}{[\text{DNA}]}\frac{1}{K} + \Delta\varepsilon \quad (1)$$

where ε_A, ε_B, and ε_F are the ratio of absorbance/[Fe(4-TMPyP)] and the absorptivities of the bound and free Fe(4-TMPyP), respectively, and $\Delta\varepsilon = \varepsilon_F - \varepsilon_B$. Accordingly, the slope and intercept of the $\varepsilon_F - \varepsilon_A$ versus $(\varepsilon_A - \varepsilon_F)/[\text{DNA}]$ plot give the binding constant, K, and $\Delta\varepsilon$. The absorbance change observed in the spectrophotometric titration curves of Fe(4-TMPyP) by DNA were consistent with the existence of two distinct interaction mechanisms in the low and high DNA concentration ranges. The corresponding binding constants were calculated to be $K_1 = (6.6 \pm 0.7) \times 10^4\ M^{-1}$ and $K_2 = (3.7 \pm 0.5) \times 10^5\ M^{-1}$, thereby giving $\varepsilon_{\text{bound I}} = 1.28 \times 10^4\ M^{-1}\ cm^{-1}$ and $\varepsilon_{\text{bound II}} = 6.84 \times 10^4\ M^{-1}\ cm^{-1}$, respectively. This was the reason why an initial decrease

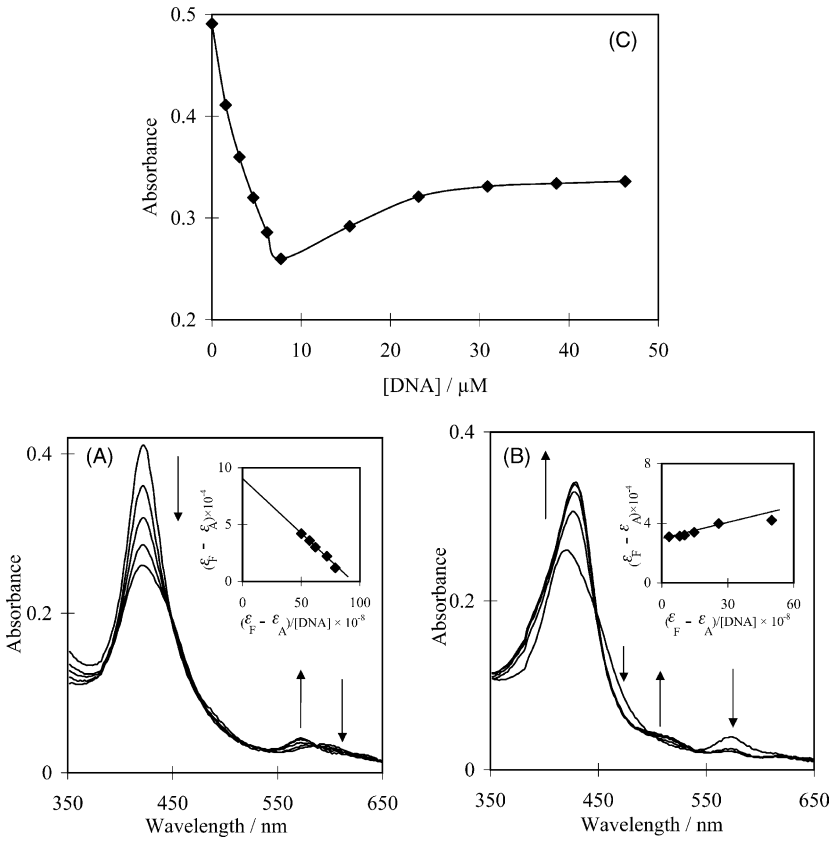

Fig. 2. UV-Vis spectral change in the titration of 5 μM Fe(4-TMPyP) with different concentrations of DNA in 1.0 mM pH 7.4 PBS. (A) Lower concentrations: 1.5, 3.0, 4.5, 6.0 and 7.5 μM st-DNA. Inset: plot of $\varepsilon_F - \varepsilon_A$ vs. $(\varepsilon_F - \varepsilon_A)$/[DNA]. (B) Higher concentrations: 7.5, 15.0, 22.5, 30.0, 38.6 and 46.3 μM st-DNA. Inset: plot of $\varepsilon_F - \varepsilon_A$ vs. $(\varepsilon_F - \varepsilon_A)$/[DNA]. (C) Plot of absorbance at 422 nm vs. DNA phosphate concentration.

and following an increase in the absorbance were observed as DNA concentration increased.

On the other hand, a constant absorption spectrum, which is identical with that of the bound II species, was observed in the large excess of DNA. In a solution containing 50-fold excess of DNA over porphyrin, The value of $6.72 \times 10^4\,M^{-1}\,cm^{-1}$ for $\varepsilon_{bound\,II}$ evaluated from the absorbance at 428 nm was in excellent agreement with $\varepsilon_{bound\,II} = 6.84 \times 10^4\,M^{-1}\,cm^{-1}$. This result further verified that the formation of bound II species was thermodynamically feasibility at excess of DNA over porphyrin.

3.2. Immobilization of Fe(4-TMPyP) in DNA-PADDA film on PGE

The mass increase due to adsorption can be estimated from the QCM frequency shift by using following Sauerbrey equation [33]:

$$\Delta F = -1.832 \times 10^8 \frac{m}{A} \quad (2)$$

where m (g) is the mass of adsorbed species, ΔF (Hz) is the frequency shift, A is the surface area of the resonator. The surface area of Au/quartz crystal electrode exposed to electrolytic solution was $0.2 \pm 0.01\,cm^2$. This meant that 1 Hz change in ΔF corresponded to 1.09 ng.

DNA is a negatively charged biological substance, while polycations PADDA and PDDA have positive charges on its backbone in the co-immobilizing polymer. Thus, DNA can combine with PADDA or PDDA (poly(diallyldimethylammonium chloride)) by coulombic attraction to form a stable multilayer film. However, a defect was observed due to the strong aggregation when preparing the DNA-PDDA, because PDDA has high positive charge density on the backbone. Thus, we chose PADDA as a polycation counter of DNA. Fig. 3 shows the time-dependent frequency change of the Au/quartz crystal. On a bare Au/quartz crystal electrode, no significant frequency change was observed on the QCM electrode (Fig. 3a). However, the DNA-PADDA modified Au/crystal electrode showed an obvious frequency decrease (Fig. 3b). The change was attributed to the entrapping of Fe(4-TMPyP) in DNA-PADDA film. In the first stage a sharp decrease of the frequency was observed. The first-order rate constant was obtained by curve fitting as a characteristic time of immobilization, τ, of 10 min. The immobilization rate constant was $34\,ng\,min^{-1}$. The total change in the frequency corresponded to an accumulation of 0.65 μg in the film after interaction with Fe(4-TMPyP) for 60 min toward a saturation value.

Electronic absorption spectrum of FePyDP modified ITO transparent electrode showed a red shift in the Soret band

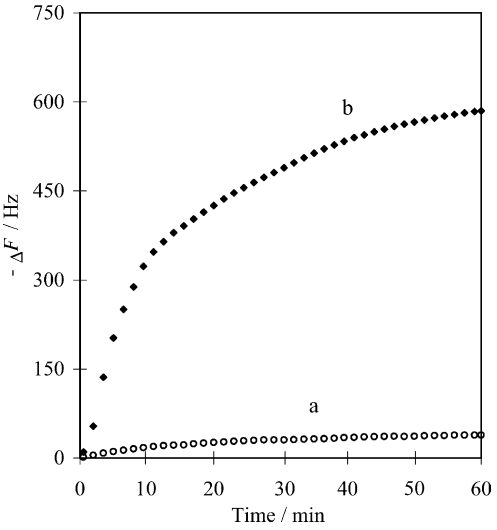

Fig. 3. In situ monitoring of the frequency decreases ($-\Delta F$) with the time for the immobilization of 2×10^{-4} M Fe(4-TMPyP) in pH 7.4 PBS onto (a) a bare Au/quartz crystal, and (b) a DNA-PADDA modified Au/quartz crystal electrode.

from 422 to 428 nm and a new absorption peak appeared at 515 nm (Fig. 4a). Obviously, bound II was formed by assembly of Fe(4-TMPyP) in DNA-PADDA film. This result was consistent with the thermodynamically stable bound II as the final species. Moreover, the binding between DNA and PADDA neutralized the negative charge of the phosphate groups in the DNA-PADDA microenvironment, especially in major groove, thus DNA minor groove produced better steric conditions for the formation of porphyrin interaction as compared with those in the major one [34].

The concentration of Fe(4-TMPyP) in FePyDP film was estimated to be 0.028 ± 0.002 M and 0.017 ± 0.001 M from

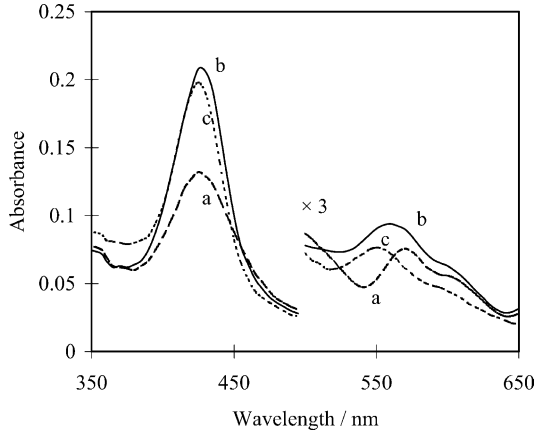

Fig. 4. Absorption spectra of FePyDP film on an optically transparent ITO electrode in pH 7.4 PBS (a) without and (b) with saturated solution of 5% NO gas. (c) Absorption spectrum of 1×10^{-4} M Fe(4-TMPyP) solution with saturated solution of 5% NO gas in an optically transparent thin layer cell which was composed of two ITO-coated glass plates with the optical pathlength of ca. 0.2 mm.

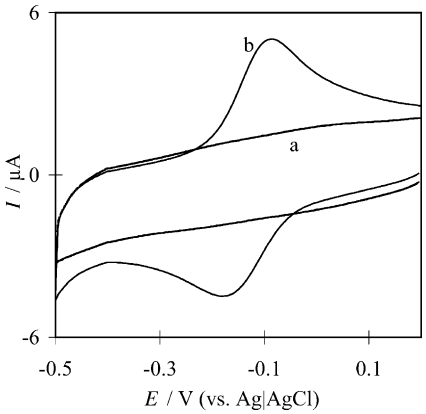

Fig. 5. Cyclic voltammograms obtained in pH 7.4 PBS at (a) DNA-PADDA film, and (b) FePyDP film modified PGE. Scan rate, 200 mV s^{-1}.

QCM and UV-Vis data by assuming the film thickness of 1.2 μm, respectively.

3.3. Electrochemical characterization of Fe(4-TMPyP)-DNA-PADDA film

In pH 7.4 PBS the FePyDP film modified electrode showed a couple of characteristic Fe^{III}/Fe^{II} redox peaks of Fe(4-TMPyP) at -0.10 and -0.17 V for a sweep rate of 200 mV s^{-1} (Fig. 5b). The peak-to-peak separation (ΔE_p) was ca. 72 mV, and the formal potential ($E^{o\prime}$), estimated by the average of anodic and cathodic peak potentials, was -0.13 V. This value was slightly higher than that determined in the same pH solution on bare PGE. In contrast, no CV peak was observed at DNA-PADDA film modified electrode under the same conditions in this potential range (Fig. 5a). These results suggested a direct electron transfer between Fe(4-TMPyP) and electrode. Fig. 6 shows the cyclic voltammograms of a multilayer FePyDP film at different scan rates. In the scan rate range of 50–1000 mV s^{-1}, The cathodic peak potential shifted to a more negative value

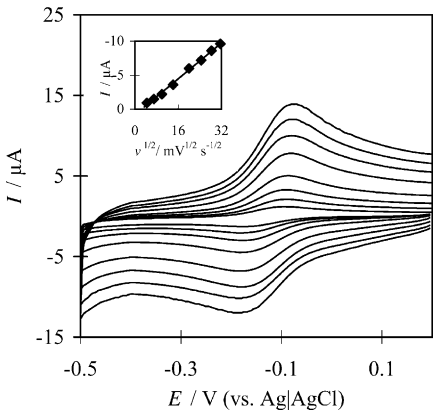

Fig. 6. Cyclic voltammograms obtained at a FePyDP film modified PG electrode in pH 7.4 PBS at various scan rates: 20, 50, 100, 200, 400, 600, 800, and 1000 mV s^{-1} (from inner to outer). Inset: plot of peak current vs. on square root of scan rate ($v^{1/2}$).

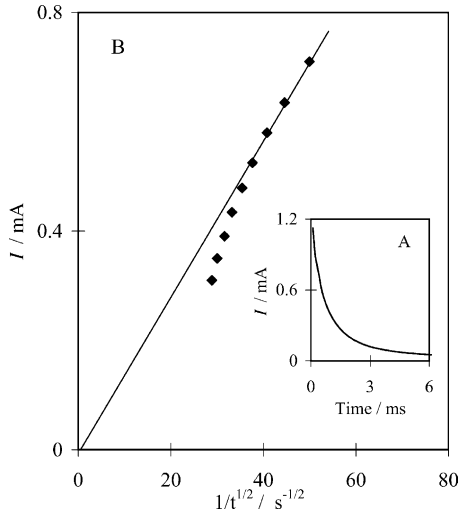

Fig. 7. Chronoamperometry obtained at a FePyDP film modified PG electrode in pH 7.4 PBS (A) current vs. time curve after application of a potential step from 0 to −500 mV vs. (Ag|AgCl). (B) Plot of i vs. $t^{-1/2}$.

with the increase of scan rate, and the peak currents were proportional to the square root of scan rate (inset of Fig. 6).

The electron transport ability in the polymer-modified electrode is typically characterized by apparent diffusion coefficients, D_{app}. Thus, we have carried out chronoamperometry experiments at a FePyDP film modified PGE in Fig. 7. $D_{app}^{1/2}C$ value which was calculated from the slopes of the i versus $t^{-1/2}$ plot was 3.2×10^{-9} mol/($s^{1/2}$ $cm^{1/2}$) by fitting the observed current-time transients to the Cottrell equation, derived from Fick's laws of diffusion: $i = nFACD_{app}^{1/2}/\pi^{1/2}t^{1/2}$ [35]. Combining this value of the concentration from UV-visible and QCM measurements, gives D_{app} value of 3.6×10^{-8} and 1.2×10^{-8} cm^2 s^{-1}, respectively. This result is consistent with the order magnitude of charge transport of 10^{-8} to 10^{-13} cm^2 s^{-1} in the ion-exchange copolymer film [36].

On the other hand, fresh DNA-PADDA film coated PGE was immersed in pH 7.4 PBS containing 0.2 mM Fe(4-TMPyP), and successive cyclic voltammetry was measured. The redox peak currents were increased with increasing in the potential sweep cycles, but reached a steady voltammogram after about 20 min. This time till the steady voltammogram was nearly same as that observed at QCM (Fig. 3). This steady voltammogram was compared with that at bare PGE (Fig. 8). The redox peak currents at DNA-PADDA film were larger than those at bare PGE and the formal potential shifted to more positive. The results in Fig. 8 are different from those at neutral 1,1′-ferrocenedimethanol where a decrease in redox peak currents and no change in the formal potential were observed between the film coated and bare PGE.

In order to clarify the effect of DNA, cyclic voltammograms of Fe(4-TMPyP) were measured in pH 7.4 PBS containing double stranded DNA and PVS (poly(vinylsulfonate)) as a simple polyanion. The experimental results clarified

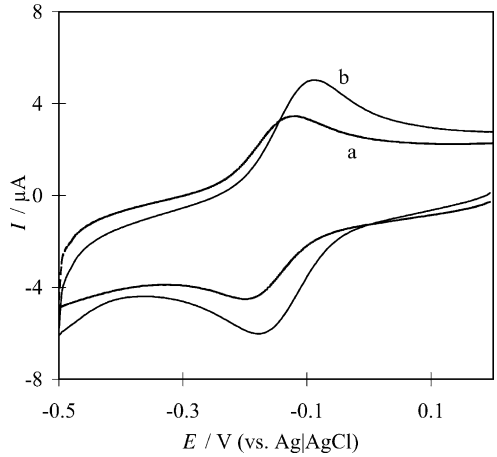

Fig. 8. Cyclic voltammograms of 2×10^{-4} M Fe(4-TMPyP) in pH 7.4 PBS at (a) bare PGE, and (b) DNA-PADDA film modified PGE. Scan rate, 200 mV s^{-1}.

that, in contrast to PVS, DNA did not inhibit the redox reaction of $Fe^{III/II}$(4-TMPyP) and O=Fe^{IV}(4-TMPyP). Indeed, DNA may convey electrons between metal-containing intercalators over relatively great distance, and enhance electron transfer of cytochrome *c* in solution in the presence of nucleic acids [37]. Thus, it was expected that Fe(4-TMPyP) molecule in FePyDP film diffuse to DNA sites near electrode surface and exchange electrons with electrode by an electron tunneling through DNA base pairs.

3.4. Catalytic reduction of NO at FePyDP elelctrode

When NO was dissolved into pH 7.4 PBS, the CV of FePyDP film modified electrode showed a new peak at −0.61 V (Fig. 9c) at the expense of Fe^{III}/Fe^{II} redox peaks. The loss current in magnitude of the Fe^{III}/Fe^{II} peak could be

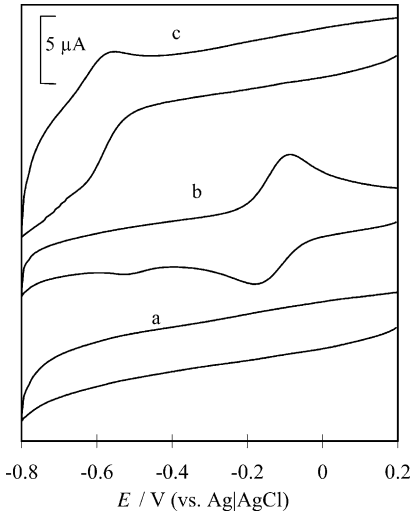

Fig. 9. Cyclic voltammograms in deareated 50 mM PBS (pH 7.4) at (a) DNA-PADDA film electrode in the presence of 82.3 μM NO, (b) and (c) FePyDP film electrode in the presence of 100 μM NO_2^- and 82.3 μM NO, respectively. Scan rate, 200 mV s^{-1}.

explained either by the direct binding of NO with Fe(III) to form a Fe(III) nitrosyl compound or by a chemical reaction between Fe(III) and NO, which removed Fe(III) species. If Fe(III) bound NO to form a stable Fe(III) nitrosyl compound, a new oxidation peak of comparable current would be expected near the redox couple of Fe^{III}/Fe^{II} for the new complex. However, the absence of such a new reduction peak suggested a mechanism other than the binding of Fe(III) with NO to form a Fe(III) nitrosyl compound. Alternatively, it should appear that other chemical process has occurred between NO and Fe(III). In our previous works, it has been reported a reductive nitrosylation as a probable pathway to explain the observed phenomenon in solution [23]. We propose a similar reduction process of Fe(III) with NO at a FePyDP film electrode, as following:

$$Fe^{III}(4\text{-TMPyP}) + 2NO + OH^- \rightarrow Fe^{II}(NO)(4\text{-TMPyP}) + HNO_2 \quad (3)$$

This reductive nitrosylation has been described for a number of heme proteins and model complexes [38].

Absorption spectrum also suggested a strong interaction between Fe(4-TMPyP) and NO when NO was added to the electrochemical cell. The absorption spectrum of Fe^{III}(4-TMPyP) in FePyDP film in pH 7.4 PBS showed a Soret band at 428 nm. After bubbling 5% NO gas up to saturation in this solution, however, it was observed that λ_{max} value was blue-shifted from 428 nm to 425 nm (Fig. 4b). Such a blue shift at the Soret band is known to be a characteristic of NO binding to iron(II) porphyrins [23]. Therefore, this result suggested that the reaction was thermodynamically favorable to form Fe^{II}(NO)(4-TMPyP). Comparing with Fig. 4c and b, the Soret band was red-shifted from 422 to 425 nm. It further suggested that the interaction with NO was not the free Fe(4-TMPyP) but Fe(4-TMPyP) bound DNA complex in a DNA-PADDA film. Fe^{II}(NO)(4-TMPyP) was stable for reduction or oxidation in the potential range of −0.6 to +0.35 V versus Ag|AgCl.

At DNA-PADDA film modified electrode the voltammogram of NO in pH 7.4 PBS showed a small current at −0.89 V. A large reductive current was observed in the presence of NO at FePyDP film modified electrode, while the redox peaks of Fe(4-TMPyP) disappeared (Fig. 9c). The large reductive current resulted from the catalytic reduction of NO by the immobilized Fe(4-TMPyP), and peak current ratio was ca. 15 for the peak current versus the noncatalytic $Fe^{III/II}$ reduction peak at the saturation concentration of 100% NO (1.8 mM). The above results indicated a high catalytic activity of iron porphyrin for NO reduction at FePyDP film modified electrode. More interestingly, an addition of nitrite into pure Fe(4-TMPyP) solution caused little change in the cyclic voltammogram (Figs. 5b and 9b). This indicated that nitrite could not be reduced at FePyDP film modified electrode in this potential range. As a conclusion, it was clarified that FePyDP film exhibited selective catalytic reduction of NO against NO_2^-.

To obtain more detailed analysis, cycle voltammetry were carried out at different pH. As increasing pH, the catalytic peak currents ($I_{cat,p}$) decreased and the catalytic peak potentials shifted to more negative potentials, which indicated proton accelerated the reduction of NO at FePyDP film modified electrode. As discussed above, the catalytic current corresponded to the reduction of ferrous-nitrosyl adduct, Fe^{II}(NO)TMPyP, to produce a nitroxyl intermediate (Eq. (4)):

$$Fe^{II}(NO)(4\text{-TMPyP}) + e^- \rightarrow Fe^{II}(NO^-)(4\text{-TMPyP}) \quad (4)$$

$$Fe^{II}(NO^-)(4\text{-TMPyP}) + H^+ \rightarrow Fe^{II}(4\text{-TMPyP}) + HNO \quad (5)$$

Such reduction of Fe^{II}-NO nitrosyl adduct to give a nitroxyl intermediate has been previously reported in the case of MbFe incorporated in DDAB film [39]. It was clear that $Fe^{II}(NO^-)$(4-TMPyP) was unstable and was irreversibly transformed into the ferrous form by a nucleophilic attack of proton [40]. The dissociation of $Fe^{II}(NO^-)$(4-TMPyP) was promoted at low pH, leading to the increase of catalytic current with decreasing pH. The pH dependence of the catalytic current suggested that the nitroxyl immediate could be decomposed by loss of HNO, which then rapidly coupled in solution to form N_2O (Eq. (6)):

$$2HNO \rightarrow N_2O + H_2O \quad (6)$$

On the other hand, cyclic voltammetry for NO reduction at FePyDP showed a dependence of the catalytic reduction current on the concentration of NO. At the saturation concentration of 100% NO (1.8 mM), the reduction peak current was 55.8 μA. This current was ca. 15 times larger than that of the noncatalytic $Fe^{III/II}$ reduction peak. This result supports an EC mechanism as shown in Eqs. (4) and (5). In a conclusion, the FePyDP film electrode displayed excellent catalytic activity for the NO reduction at −0.61 V versus Ag|AgCl. The whole reduction process of NO was a typical EC mechanism.

3.5. Amperometric detection of nitric oxide

Quantification of NO using the proposed FePyDP modified electrode was carried out by a chronoamperometry at −700 mV. All measurements were performed with strict exclusion of molecular oxygen, and the electrodes have been conditioned by means of cyclic voltammetry prior to the measurement. The inset in Fig. 10 shows typical amperometric response with successive additions of NO. The sensor showed a response time of 1.5 s after NO addition, indicating a fast response to NO reduction. The calibration curve of the sensor showed a linear response in NO concentration range of 1.0×10^{-7} to 9.0×10^{-5} M with a correlation coefficient of 0.9987 (Fig. 10). From the slope of 0.049 μA μM^{-1}, the detection limit calculated at a signal-to-noise ratio of 3 was 3.0×10^{-8} M.

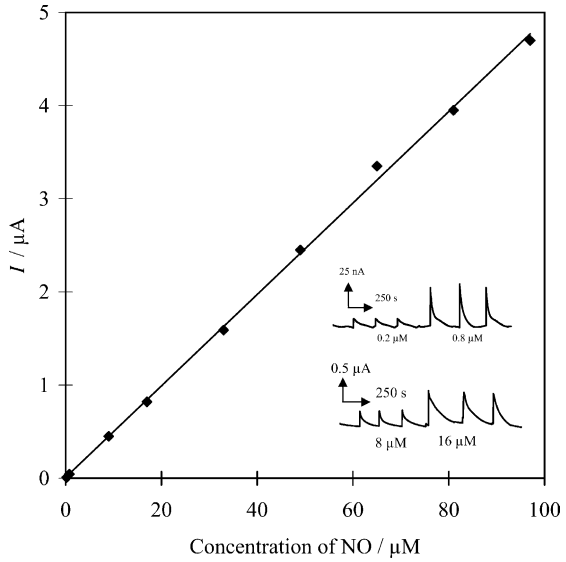

Fig. 10. Calibration curve for amperometric determination of NO at a FePyDP modified PGE. Applied potential, −700 mV vs. (Ag|AgCl). Inset: amperometric response upon injection of NO solution.

Since the estimated amount of NO released from single cell is about 1–200 attomol, i.e. 2×10^{-4} to 1×10^{-6} M, the detection limit of the proposed sensor would be suitable for in vivo determination of NO. The stability of sensor was good. It was used for at least two week without obvious decrease in the response to NO, when the sensors were kept in a phosphate buffer solution with pH 7.4 at 4 °C. Reproducibility as the NO sensor at different electrodes ($n = 11$) was investigated by injections of 8 μM NO. The relative standard deviation (RSD) of catalytic current was 6.3%. It was clarified that this FePyDP film modified electrode showed a good reproducibility for the response of NO.

4. Conclusions

This work utilizes the supramolecular interaction between Fe(4-TMPyP) and DNA template to form a stable FePyDP film by assembling water-soluble Fe(4-TMPyP) into DNA-PADDA film. The direct electron transfer involving a well reversible Fe^{III}/Fe^{II} couple was observed via the double-strand of DNA. The modified electrode displays excellent catalytic activity for the NO reduction at −0.61 V versus Ag|AgCl, leading to a NO biosensor. This response represents a diminution of about 280 mV in the potential of NO reduction at a bare PGE. It is expected that the supramolecular assembly based on cationic porphyrins and DNA template could be widely applied as conductive biomaterial and provide new insights on the water-soluble porphyrin modified electrode as third reagentless biosensor.

References

[1] S. Kim, G. Deinum, M.T. Gardner, M.A. Marletta, G.T. Babcock, J. Am. Chem. Soc. 118 (1996) 8769.
[2] S. Pfeiffer, B. Mayer, B. Hemmens, Angew. Chem. Int. Ed. 38 (1999) 1714.
[3] S. Moncada, R.M.J. Palmer, E.A. Higgs, Pharmacol. Rev. 43 (1991) 109.
[4] T. Malinski, Z. Taha, Nature 358 (1992) 676.
[5] F. Bedioui, S. Trevin, V. Albin, M.G.G. Villegas, J. Devynck, Anal. Chim. Acta 341 (1997) 177.
[6] S.L. Vilakazi, T. Nyokong, Electrochim. Acta 46 (2000) 453.
[7] N. Diab, W. Schuhmann, Electrochim. Acta 47 (2001) 265.
[8] A. Ciszewski, E. Kubaszewski, L. Lozynski, Electroanalysis 8 (1996) 261.
[9] J. Hayon, D. Ozer, J. Rishpon, A. Bettelheim, J. Chem. Soc. Chem. Commun. (1994) 619.
[10] A.V. Kashevskii, A.Y. Safronov, O. Ikeda, J. Electroanal. Chem. 510 (2001) 86.
[11] A.V. Kashevskii, J. Lei, A.Y. Safronov, O. Ikeda, J. Electroanal. Chem. 531 (2002) 71.
[12] R.F. Pasternack, E.J. Gibbs, J.J. Villafranca, Biochemistry 22 (1983) 2406.
[13] N.E. Makundan, G. Petho, D.W. Dixon, L.G. Marzilli, Inorg. Chem. 34 (1995) 3677.
[14] A.B. Guliaev, N.B. Leontis, Biochemistry 38 (1999) 15425.
[15] J. Lang, M.H. Liu, J. Phys. Chem. B103 (1999) 11393.
[16] B. Giese, A. Biland, Chem. Commun. (2002) 667.
[17] H. Nakayama, H. Ohno, Y. Okahata, Chem. Commun. (2001) 2300.
[18] T. Hirao, A. Nomoto, S. Yamazaki, A. Ogawa, T. Moriuchi, Tetrahedron Lett. 39 (1998) 4295.
[19] S.O. Kelley, N.M. Jackson, M.G. Hill, J.K. Barton, Angew. Chem. Int. Ed. 38 (1999) 941.
[20] M. Aoudia, M.A.J. Rodgers, J. Am. Chem. Soc. 119 (1997) 12859.
[21] Y.M. Lvov, Z. Lu, J.B. Schenkman, X. Zu, J.F. Rusling, J. Am. Chem. Soc. 120 (1998) 4073.
[22] A.C. Onuoha, J.F. Rusling, Langmuir 11 (1995) 3296.
[23] N.S. Trofimova, A.Y. Safronov, O. Ikeda, Inorg. Chem. 42 (2003) 1945.
[24] R.F. Pasternack, H. Lee, P. Makel, C. Spencer, J. Inorg. Nucl. Chem. 39 (1997) 1865.
[25] F. Bedioui, Y. Bouhier, C. Sorel, J. Devynck, L. Coche-Guerente, A. Deronzier, J.C. Moutet, Electrochim. Acta 38 (1993) 2485.
[26] D.R. Lide (Ed.), CRC Handbook of Chemistry and Physics, Section 6-3, 76th ed., CRC Press, Boca Raton, FL, 1995.
[27] J. Brandrup, E. Immergut, Polymer Handbook, Part 5, Wiley, New York, Chichester, Brisbane, Toronto, 1975.
[28] T.E. Creighton, Protein Structure: A Practical Approach, IRL Press, Oxford, New York, Tokyo, 1990, p. 43.
[29] K. Araki, C.A. Silva, H.E. Toma, L.H. Catalani, M.H.G. Medeiros, P.D. Mascio, J. Inorg. Biochem. 78 (2000) 269.
[30] R.A. Vilaplana, F.G. Vilchez, R.F. Pasternack, J. Chem. Soc., Dalton Trans. (1991) 1831.
[31] R. Kuroda, H. Tanaka, J. Chem. Soc., Chem. Commun. (1994) 1575.
[32] R. Lavery, B. Pullman, J. Biomol. Struct. Dyn. 2 (1985) 1021.
[33] G.Z. Sauerbrey, Physics 155 (1959) 206.
[34] I.E. Borissevitch, S.C.M. Gandini, J. Photochem. Photobiol. B: Biol. 43 (1998) 112.
[35] R.W. Murray, Molecular Design of Electrode Surfaces, vol. XXII, Wiley, New York, Chichester, Brisbane, Toronto, Singapore, 1992 (Chapter 4).
[36] J. Facci, R.W. Murray, J. Phys. Chem. 85 (1981) 2870.
[37] O. Ikeda, Y. Shirota, T. Sakurai, J. Electroanal. Chem. 287 (1990) 179.
[38] M. Hoshino, M. Maeda, R. Konishi, H. Seki, P.C. Ford, J. Am. Chem. Soc. 118 (1996) 5702.
[39] M. Bayachou, R. Lin, W. Cho, P.J. Farmer, J. Am. Chem. Soc. 120 (1998) 9888.
[40] M.H. Barley, M.R. Rhodes, T.J. Meyer, Inorg. Chem. 26 (1987) 1746.